

# CAPTURE OF 10–100 keV NEUTRONS IN ISOTOPES OF TITANIUM

By G. J. BROOMHALL\*

[Manuscript received 24 August 1971]

## *Abstract*

Gamma ray spectra are presented as functions of neutron energy for capture of 10–100 keV neutrons in natural titanium. The spectra are dominated by transitions to the first, third, and fifth excited states of  $^{49}\text{Ti}$  which show strong fluctuations with neutron energy. The nature of these fluctuations and their relation to the nature of the capture process is discussed. A small but measurable strength in the transition to the  $7/2^-$  ground state of  $^{49}\text{Ti}$  has been observed and this is interpreted as evidence for the existence of a d-wave resonance in the reaction  $^{48}\text{Ti}(n, \gamma)^{49}\text{Ti}$  at 39 keV. Transitions at 8260 and 8380 keV are assigned to capture in  $^{47}\text{Ti}$ .

## I. INTRODUCTION

The  $\gamma$ -ray spectrum following thermal capture in titanium is dominated by three high energy E1 transitions to  $3/2^-$  and  $1/2^-$  states in  $^{49}\text{Ti}$ , a phenomenon which is fairly common for spectra from nuclei in the mass range  $A = 40-70$ . These low lying states occur near the known binding energy for the 2p neutron orbital, and it has been suggested by Lane and Lynn (1960) that a fast capture process is involved with single-particle transitions directly from the s-wave capturing state to the final p-state. Considerable experimental effort has been directed towards defining the role of simple configurations in the capture mechanism.

Measurements of  $\gamma$ -ray spectra from keV neutron capture in natural titanium have been reported by Bird, Kenny, and Allen (1968), Allen, Bird, and Kenny (1969), and Broomhall (1969). The present paper contains a detailed analysis and evaluation of these results. In the series of experiments described the study of the titanium  $\gamma$ -rays has been extended to the keV resonance region where there are a number of strong s-wave resonances, contributions from which could make up a large fraction of the thermal capture cross section. Spectra from these resonances were measured using both NaI(Tl) and Ge(Li) detectors and relative partial capture widths were calculated.

## II. RESULTS

Various sets of data were obtained using both NaI(Tl) and Ge(Li) detectors. System parameters characterizing the sets to be discussed below are summarized in Table 1.

### *(a) NaI Data*

The experimental system used has been described by Bird, Gibbons, and Good (1962), and the experiments are summarized in sets 1 and 2 of Table 1. For data set 1, time-of-flight measurements were used to separate the neutron events, centred around

\* School of Physics, University of Melbourne; present address: AAEC Research Establishment, Private Mail Bag, Sutherland, N.S.W. 2232.

an energy of 30 keV, from background. A 10 cm diameter lead collimator in front of the NaI detector was used for best  $\gamma$ -ray resolution and line shape. The  $\gamma$ -ray intensities obtained by a least squares fit of standard line shapes are listed in Table 2. Figure 1 shows peak positions of these fitted shapes, together with the line shape for a 6.75 MeV  $\gamma$ -ray. Isotopic allocation other than for  $^{49}\text{Ti}$  was made by comparison with published thermal data (Bartholomew *et al.* 1967). The 8.14 MeV peak is confirmed as the  $^{49}\text{Ti}$  ground state from set 2.

In set 2, two-parameter analysis gave  $\gamma$ -ray pulse heights for 16 windows on the time spectrum (Fig. 2). All spectra show a background peak at approximately 7.6 MeV which results from neutron capture in the steel detector support. In the spectra for neutron energies near 35 and 42 keV there is a peak at 8.14 MeV which was identified as the ground state transition in  $^{49}\text{Ti}$ . The  $\gamma$ -ray intensities for the

TABLE 1  
SUMMARY OF EXPERIMENTAL PARAMETERS

Parameter	Data set 1*	Data set 2†	Data set 3‡	Data set 4§
Location of experiment	ORNL	ORNL	AAEC	AAEC
Detector	30 × 25 cm NaI(Tl)	30 × 25 cm NaI(Tl)	30 cm <sup>3</sup> Ge(Li)	30 cm <sup>3</sup> Ge(Li)
Flight path (cm)	15	51	50	43
$E_n$ range (keV)	18–46	5–95	5–80	5–85
$E_\gamma$ range (MeV)	2–9.5	5.5–9.5	5–7	5–9
$\gamma$ -ray spectra obtained	1	14	4	5
Timing resolution (ns)	14	14	25	28
$\gamma$ -ray resolution (keV)	250	250	9	17

\* Bird, Gibbons, and Good (1962).

‡ Bird, Kenny, and Allen (1968).

† Bird, Gibbons, and Good (1962); Broomhall (1969).

§ Allen, Bird, and Kenny (1969).

various regions of neutron energy are listed in Table 3. Relative partial cross sections were obtained by comparison with the capture yield from an indium target (Fig. 3). However, no allowance was made for multiple scattering in the very thick ( $\sim 2.5$  cm) target used.

#### (b) *Ge(Li) Data*

The detection system and geometry used in this case have been described by Allen (1968). The  $\gamma$ -ray energy resolution of the Ge(Li) detector is sufficient to separate the thermal peak from the keV resonance peaks. In order to separate further the effects of the neutron resonances, six windows in the time-of-flight spectrum were selected by digital techniques. The background-subtracted spectra showing the three strongest  $\gamma$ -rays for each time-of-flight interval as well as the spectrum summed over all neutron energies are presented in Figure 4. The shift in peak position from D5 to D2 (i.e. from low to high neutron energy) and the structure in the summed spectrum are clearly seen. The high energy end of each spectrum is plotted separately in Figure 5. The transition to the ground state of  $^{49}\text{Ti}$  occurs at a neutron energy of 39 keV (Fig. 5). The assignment to  $^{47}\text{Ti}+n$  of the two higher energy peaks was made on the basis of recent thermal data for that isotope (Fettweis and Saidane 1969; Tripathi, Blichert, and Borevings 1969).

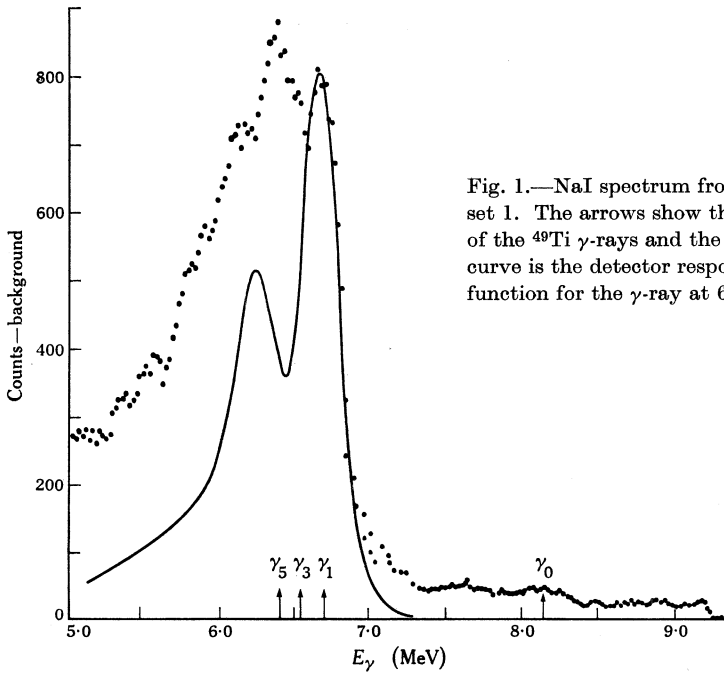


Fig. 1.—NaI spectrum from data set 1. The arrows show the positions of the  $^{49}\text{Ti}$   $\gamma$ -rays and the solid curve is the detector response function for the  $\gamma$ -ray at 6.75 MeV.

TABLE 2  
NaI RESULTS FROM DATA SET 1

$$\text{Normalization } \sum_{6.41}^{6.75} I_{\gamma}(\text{keV}) = \sum_{6.41}^{6.75} I_{\gamma}(\text{thermal}) = 76\% \text{ (natural element)}$$

$E_{\gamma}$ (MeV)	Thermal*	$I_{\gamma}$	Emitting isotope	$E_{\gamma}$ (MeV)	18-46 keV $I_{\gamma}$ (rel.)
9.376	0.08		$^{50}\text{Ti}$	9.4	$1.4 \pm 0.3$
9.189	0.08		$^{48}\text{Ti}$	9.1	$0.8 \pm 0.3$
—	—		Unassigned	8.6	$0.8 \pm 0.3$
8.342	0.05		$^{48}\text{Ti}$ , $^{50}\text{Ti}$	8.32	$1.7 \pm 0.6$
8.146	—		$^{49}\text{Ti}$	8.14	$1.2 \pm 0.6$
6.753	41.0		$^{49}\text{Ti}$	6.74	$39 \pm 1$
6.550	5.9		$^{49}\text{Ti}$	6.55	$13 \pm 2$
6.413	29.0		$^{49}\text{Ti}$	6.41	$24 \pm 1$

\* Bartholomew *et al.* (1967).

The data shown in Figures 4 and 5 are from set 4 of Table 1 and were analysed by Gaussian peak fitting to give  $\gamma$ -ray intensities after correction for incident neutron flux shape (Table 4). The results in Tables 2, 3, and 4 are presented as relative  $\gamma$ -ray intensities and were normalized so that the sum over neutron energy for the three strong transitions in  $^{49}\text{Ti}$ , 6.753, 6.550, and 6.413 MeV, was equal to 76 photons per 100 captures, the value obtained by Bartholomew *et al.* (1967) for thermal capture.

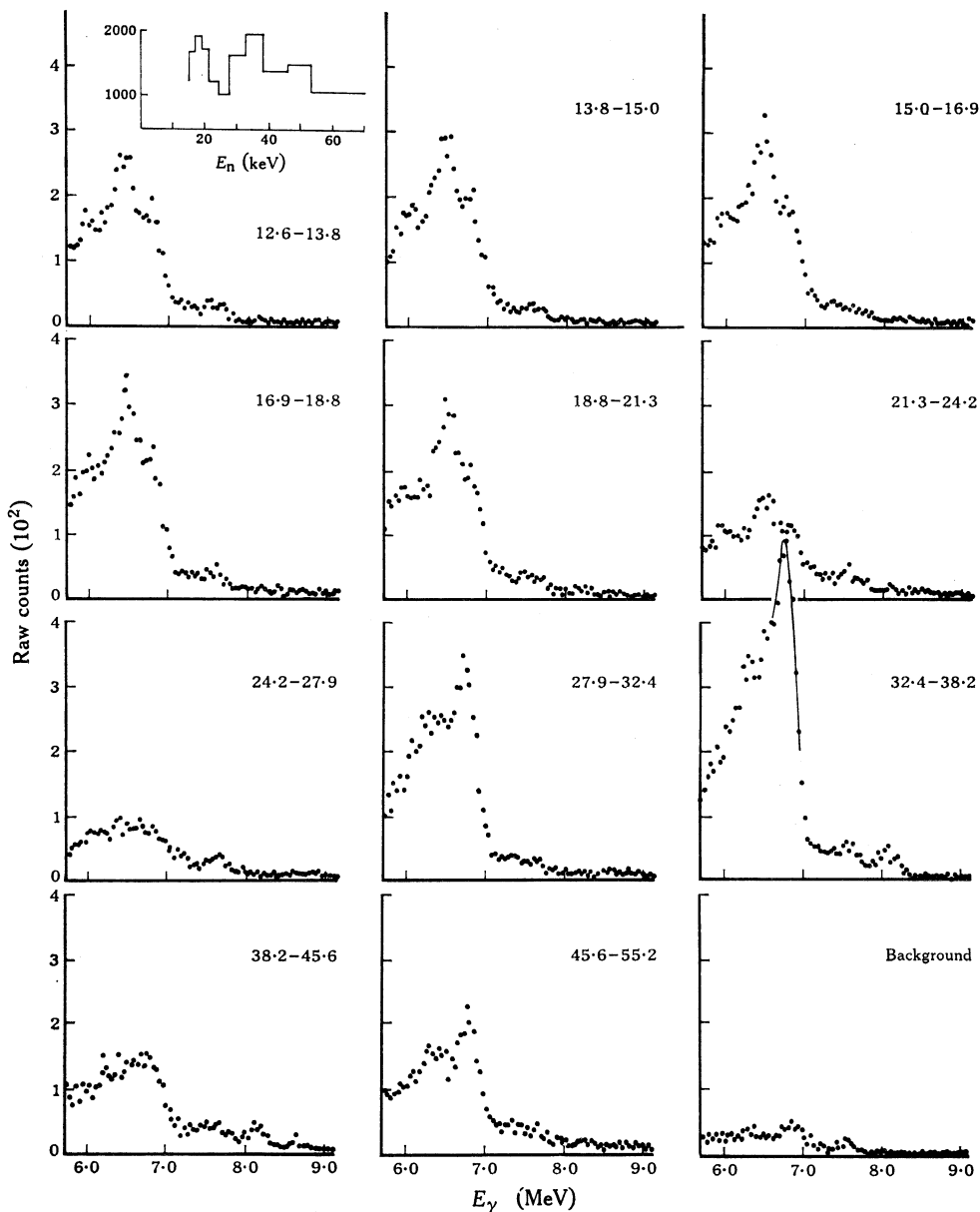


Fig. 2.—NaI spectra from data set 2 for the indicated ranges of  $E_n$  (keV). The ground state transition at 8.14 MeV is evident in the region  $E_n = 32.4$ –45.6 keV. The inset at top left shows the time-of-flight spectrum.

TABLE 3  
NaI RESULTS FROM DATA SET 2

Line No.	Final state in $^{49}\text{Ti}$ $J^\pi$	$E_\gamma$ (MeV)	$I_\gamma(\text{thermal})^*$	$\sum I_\gamma(\text{keV}) = \sum I_\gamma(\text{thermal}) = 76\%$ (natural element)		$I_\gamma(\text{rel.})$ for $E_n$ range (keV)								$\sum E_n$			
				6-41	6-75	13.8	15.0	16.9	18.8	21.3	24.2	27.9	32.4	38.2	45.6	55.2	67.3
0	7/2-	8.15	—	0.02	0.02	0.02	0.02	0.02	0.02	0.02	0.02	0.04	0.25	0.24	0.04	0.02	0.6
1	3/2-	6.75	41.0	5.29	6.24	5.83	3.75	2.08	0.35	0.29	1.85	2.85	0.35	0.64	0.39	36.0	
3	3/2-	6.55	5.9	0.04	0.04	0.28	0.41	2.36	1.28	0.20	0.80	1.20	0.28	0.08	0.05	7.3	
5	1/2-	6.41	29.0	6.18	6.60	6.44	4.92	1.98	0.20	0.10	0.08	0.13	0.08	0.18	0.16	32.5	

\* Bartholomew *et al.* (1967).

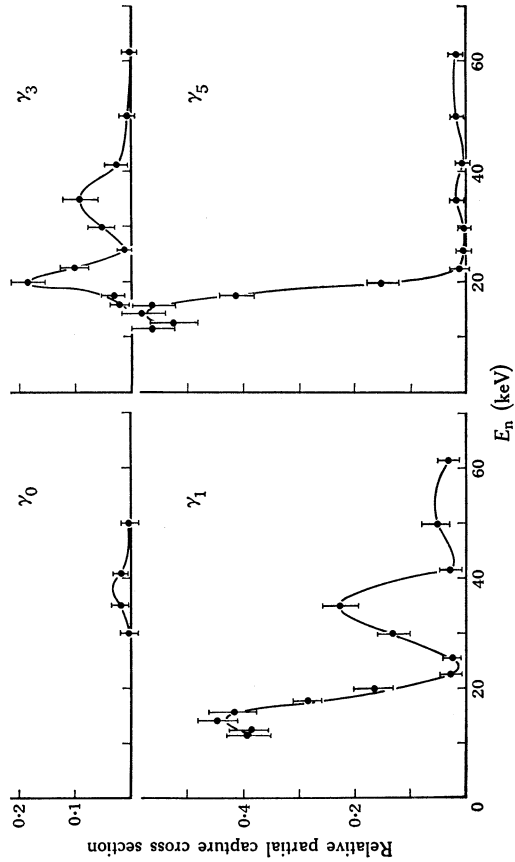


Fig. 3.—Data from set 2 reduced to relative partial capture cross sections by reference to an indium standard for the four transitions in  $^{49}\text{Ti}$ .

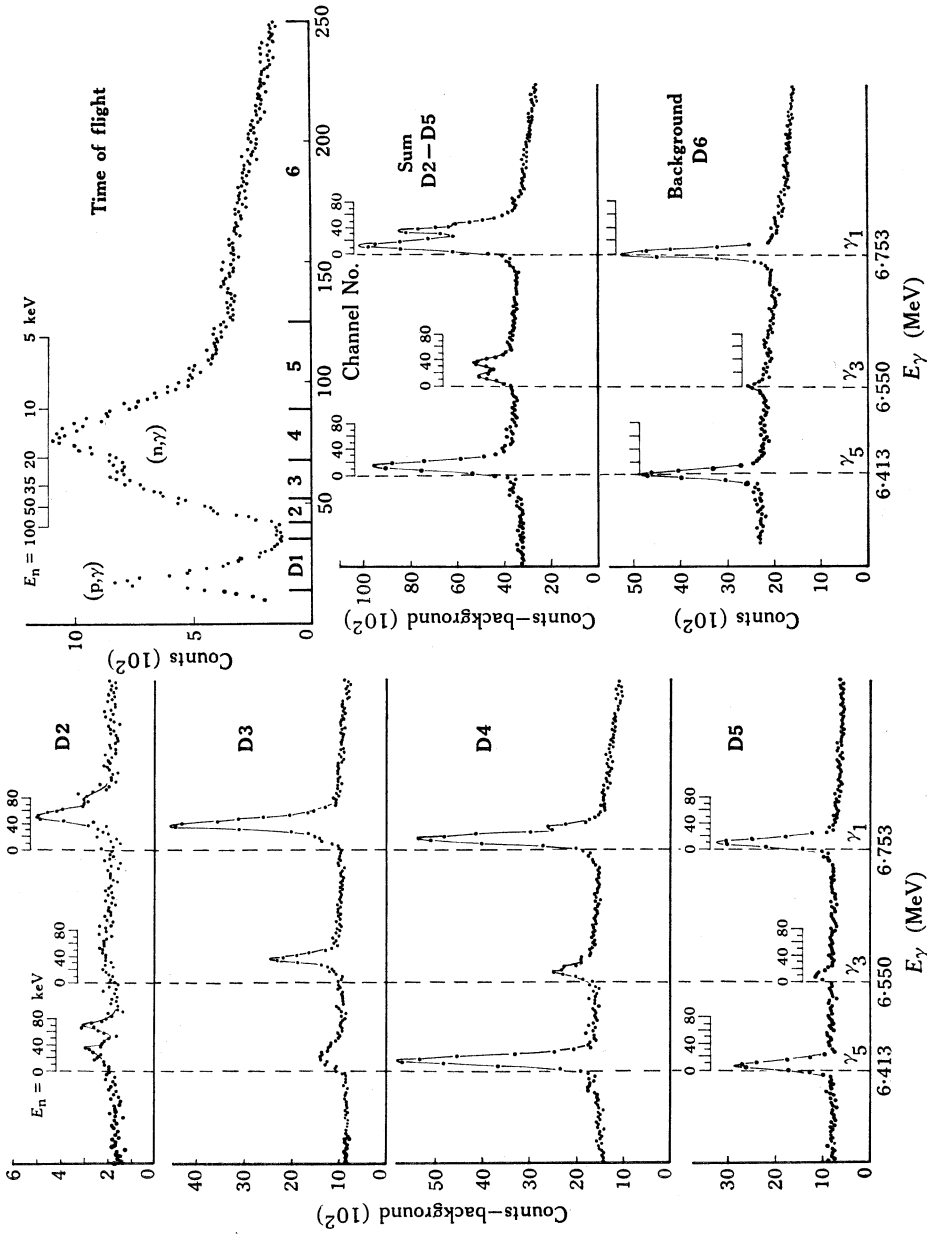


Fig. 4.—Ge(Li) spectra from data set 4 for the  $\gamma_1$ ,  $\gamma_3$ , and  $\gamma_5$  transitions in  $^{49}\text{Ti}$ . Also shown is the time-of-flight spectrum with the positions of the digital windows.

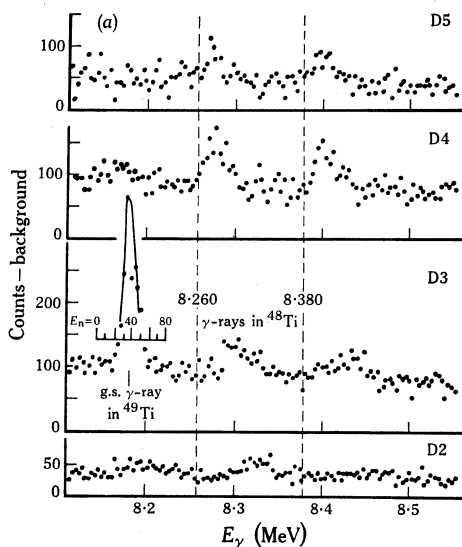


Fig. 5.—Showing (a) the high energy end of the spectra of Figure 4 with the ground state transition in  $^{49}\text{Ti}$  together with the two transitions in  $^{48}\text{Ti}$ , and (b) the positions and strengths of known resonances in  $^{47}\text{Ti}$  (Goldberg *et al.* 1966).

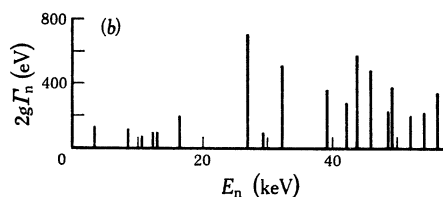


TABLE 4

Ge(Li) RESULTS FROM DATA SET 4

$6.753$                        $6.753$   
 Normalization  $\Sigma I_{\gamma}(\text{keV}) = \Sigma I_{\gamma}(\text{thermal}) = 76\%$  (natural element)  
 $6.413$                        $6.413$

Ti isotope	$E_r$ (keV)	Final state*		$I_{\gamma}(\text{thermal})$	$I_{\gamma}(\text{rel.})$ for $E_n$ (keV)					
		$l_n, J_f^{\pi}$	$E_{\gamma}$ (MeV)		14	37	39	53	76	$\Sigma E_n$
48			8.40							2.0
48			8.28							1.5
47, 50			7.08							1.0
49		3, 7/2 <sup>-</sup>	8.146	—	0.02	0.02	0.47	0.02	0.02	0.5
49	1376	1, 3/2 <sup>-</sup>	6.753	41.0	26.5	8.6	—	2.6	0.3	37.0
49	1538	—	—	—	—	—	—	—	—	—
49	1583	3/2 <sup>-</sup>	6.550	5.9	5.9	2.7	—	0.05	0.05	7.7
49	1618	—	—	—	—	—	—	—	—	—
49	1717	1, 1/2 <sup>-</sup>	6.413	29.0	29.0	1.0	—	0.2	0.3	32.0
$E_r$ (keV):					17.3,	37	—	52.5	74.2	
					22.0					
$\Gamma_n$ (keV):†					7.5,	1.7	—	3.0	0.5	
					0.5					

\* Bartholomew *et al.* (1967).

† Goldberg *et al.* (1966).

### III. DISCUSSION

#### (a) Neutron Resonances

There are five known s-wave resonances in  $^{48}\text{Ti}$  in the region 5–75 keV (Table 4). The capture data show definite peaks at approximately these resonance energies (Figs. 3 and 4). The most interesting feature of the peak structure is the predominance (approximately 80% of the total capture events) of capture between 5 and 20 keV.

Bird, Kenny, and Allen (1968) and Allen, Bird, and Kenny (1969) have analysed this region in terms of two resonances at 10 and 17 keV. However, because of the difficulty in estimating the effect on shape of multiple scattering from the large resonance at 17 keV ( $\Gamma_n = 7.5$  keV) in the very thick target used, the present analysis (Table 4) used a single peak which may contain more than one resonance. The explanation of the results in terms of known s-wave resonances, however, requires the total capture width of the 17 keV resonance to be in the range 3–7 eV which is greater than the largest value of  $\Gamma_\gamma$  reported in this region (Fig. 6).

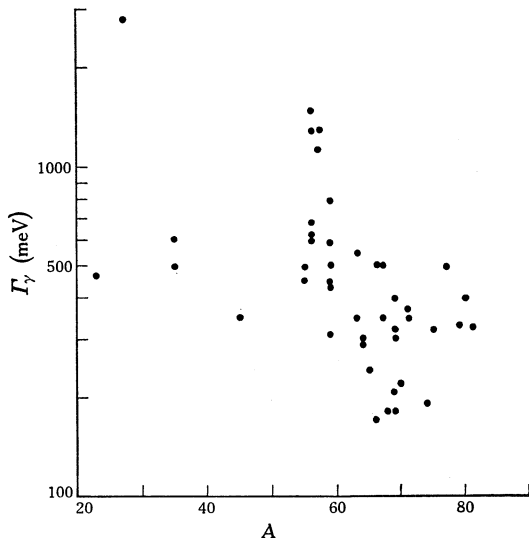


Fig. 6.—Measured values of  $\Gamma_\gamma$  plotted against atomic mass for the mass region 20–80.

### (b) Gamma Ray Spectra

The  $\gamma$ -ray spectrum following thermal capture in natural titanium is dominated by transitions to states in  $^{49}\text{Ti}$  at 1376 ( $3/2^-$ ), 1583 ( $3/2^-$ ), and 1717 ( $1/2^-$ ) keV. These contribute 76% of the total transition strength in the natural element. The  $\gamma$ -ray spectrum following keV capture is very similar so that it is possible that thermal capture is determined by the wings of the keV resonances. It is clear that the strong s-wave resonances decay by single-particle transitions to 2p states, but with the  $2p_{3/2}$  strength shared between two levels in the ratio of approximately 5 : 1. This is consistent with (d, p) results, which are discussed in Section III(d).

Transitions to positive parity states were not observed, in contrast to the case of calcium (Chan and Bird 1971), where the observation of these transitions indicates the presence of p-wave capture.

The ground state ( $7/2^-$ ) transition observed at a neutron energy of 39 keV accounts for 25% or less of the capture at this energy. However, the wide s-wave resonance at 37 keV contributes to the  $3/2^-$  and  $1/2^-$  state transitions. High resolution capture cross section measurements (Allen and Macklin 1970) show numerous narrow resonances superimposed on the broad s-wave resonances. Multipolarity considerations indicate that the best explanation of the  $7/2^-$  transition is a d-wave resonance

( $J^\pi = 5/2^+$ ) or possibly a p-wave  $3/2^-$  resonance. Calculation of the single-particle dipole matrix elements using harmonic oscillator wavefunctions for the transitions  $2d_{5/2} \rightarrow 2p_{3/2}$  and  $2d_{5/2} \rightarrow 1f_{3/2}$  shows that the transition probabilities should be equal to within 25% (Spicer, personal communication). This is compatible with the observations, but measurements of transition rates for the new resonance and angular distribution measurements are needed to confirm the d-wave interpretation.

(c) *Reduced Widths*

The reduced widths for E1 transitions were calculated in the usual way (Bartholomew 1961). For titanium, the average resonance spacing ( $\bar{D}$ ) can be estimated, but  $\Gamma_\gamma$  has not been measured for any resonance. Figure 6 shows existing  $\Gamma_\gamma$  data for resonances of nuclei in the mass range  $20 < A < 80$ . Because of the lack of data below mass 55 and the large fluctuations in the existing data, it is difficult to predict values for the lighter nuclei. However, there is a general trend towards higher  $\Gamma_\gamma$  values for decreasing  $A$ . Moreover, for lighter nuclei the rate of increase of the level density with excitation energy is considerably slower than for the heavier

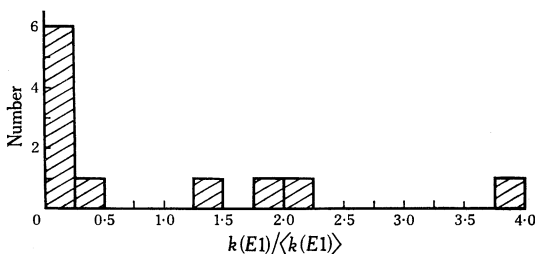


Fig. 7.—Frequency histogram for the  $\gamma_1, \gamma_3,$  and  $\gamma_5$  transitions in  $^{49}\text{Ti}$ .

nuclei. This suggests considerable fluctuations in the value of  $\Gamma_\gamma$  from resonance to resonance. This type of fluctuation has been observed for  $^{59}\text{Co}$  (Moxon 1965), where  $\Gamma_\gamma$  varies from 0.22 to 1.00 eV for the first 15 resonances. Because of the smaller number of transitions occurring in  $^{49}\text{Ti}$  even greater fluctuations in  $\Gamma_\gamma$  can be expected.

Using the data in Figure 6 and allowing for the possibility of fluctuations in  $\Gamma_\gamma$ , it is still apparent that  $\Gamma_\gamma$  is very much less than  $\Gamma_n$  for the s-wave resonances in  $^{48}\text{Ti}$ . Therefore the area under a resonance in a partial capture cross section will be proportional to the partial radiative width  $\Gamma_{\gamma i}$  for that resonance if multiple scattering effects are ignored. Reduced widths were therefore calculated from the observed intensities after correction for the variation of the number of incident neutrons as a function of neutron energy.

A frequency histogram for the calculated reduced widths is shown in Figure 7. Using the method of maximum likelihood, an estimate of  $\nu = 0.9$  was obtained for the number of degrees of freedom of the chi-squared distribution required to fit these data. In this respect therefore the large s-wave resonances behave according to a statistical model of the nucleus. However, the relative values of the total radiation widths obtained by summing corrected intensities for each resonance do, in fact, vary by a factor of 10 or more. They also show correlation with values of  $\Gamma_n$  (see Table 4).

*(d) Comparison with (d, p) Results*

For even-even target nuclei, correlations between the reduced widths of primary E1 transitions following thermal and low energy resonance capture and (d, p) strengths can give an indication of the importance of single-particle effects in the capture mechanism. The correlation coefficient  $\rho$  is given by

$$\rho = \frac{\sum_i (x_i - \bar{x})(y_i - \bar{y})}{\left( \sum_i (x_i - \bar{x})^2 \sum_i (y_i - \bar{y})^2 \right)^{\frac{1}{2}}},$$

where  $x_i$  and  $y_i$  are the reduced gamma and (d, p) widths for the transition to the  $i$ th final state. Using the average keV results from Tables 3 and 4, high positive correlation coefficients are observed in all three cases:

$$+0.87\{\text{thermal}-(d, p)\}; \quad +0.99\{\text{keV}-(d, p)\}; \quad +0.91\{\text{keV}-\text{thermal}\}.$$

This indicates that single-particle configurations play a very important role. Although only three transitions are involved these results suggest that channel capture may make an important contribution. If channel capture dominates, there should also be a correlation between the scattering and capture widths. The results in Table 4 give a correlation coefficient of  $+0.93$  which is consistent with this interpretation.

*(e) Resonances in  $^{47}\text{Ti}+n$* 

Two transitions at  $8260 \pm 5$  and  $8380 \pm 5$  keV have been assigned to  $^{48}\text{Ti}$  (Fig. 5(a)). The gross neutron resonance structure of these transitions follows the same pattern and shows peaks at 12, 28, 50, and 64 keV. Known resonances in  $^{47}\text{Ti}+n$  are shown schematically in Figure 5(b). The tendency for the resonance strength to group at around 10, 28, 45, and 60 keV indicates that the transitions were correctly assigned. Furthermore, because the neutron peak structure is the same and peak intensities are similar, it is most likely that the  $\gamma$ -rays observed are E1 transitions from  $3^-$  s-wave capturing resonances to a  $2^+$  level at 3367 keV and a  $4^+$  level at 3240 keV in  $^{48}\text{Ti}$ . This favours the spin assignments made by Kavaloski and Kossler (1969) and Fettweis and Saidane (1969).

## IV. CONCLUSIONS

Kilo-electron-volt capture in  $^{48}\text{Ti}$  is dominated by three large s-wave resonances at 17, 37, and 52 keV; the largest at 17 keV ( $\Gamma = 7.5$  keV) contributes approximately 80% of all capture events in these experiments.  $\Gamma_\gamma$  for this resonance was estimated to be in the range 3–7 eV. The close similarity between thermal and keV spectra shows that the thermal capture cross section is dominated by contributions from the wings of the three large s-wave resonances. A strong positive correlation with (d, p) results shows that transitions to single-neutron p-states is a dominant process. Furthermore, the positive correlation between  $\Gamma_n$  and the observed transition strengths suggests the influence of the channel capture process. Although there is no evidence for a strong p- or d-wave cross section over the energy region studied, a possible d-wave resonance in  $^{48}\text{Ti}$  has been observed at 39 keV.

## V. ACKNOWLEDGMENTS

I would like to thank Dr. J. R. Bird, Dr. M. J. Kenny, Mr. B. J. Allen, and the staff of the 3 MeV Accelerator Group for their invaluable help, and the Australian Institute for Nuclear Science and Engineering for the research scholarship which enabled me to carry out this work.

## VI. REFERENCES

- ALLEN, B. J. (1968).—AAEC Rep. No. TM 462.
- ALLEN, B. J., BIRD, J. R., and KENNY, M. J. (1969).—AAEC Rep. No. E 200.
- ALLEN, B. J., and MACKLIN, R. L. (1970).—*Bull. Am. phys. Soc.* **15**, 1667.
- BARTHOLOMEW, G. A. (1961).—*A. Rev. nucl. Sci.* **11**, 259.
- BARTHOLOMEW, G. A., *et al.* (1967).—*Nucl. Data A* **3**(4–6), 466.
- BIRD, J. R., GIBBONS, J. H., and GOOD, W. M. (1962).—*Phys. Lett.* **1**, 262.
- BIRD, J. R., KENNY, M. J., and ALLEN, B. J. (1968).—*Phys. Lett. B* **27**, 638.
- BROOMHALL, G. J. (1969).—Proc. Int. Conf. on Properties of Nuclear States, Montreal, p. 700.
- CHAN, D. M. H., and BIRD, J. R. (1971).—*Aust. J. Phys.* **24**, 671.
- FETTWEIS, P., and SAIDANE, M. (1969).—*Nucl. Phys. A* **139**, 113.
- GOLDBERG, M. D., MUGHABGHAB, S. F., PUROHIT, S. N., MAGURNO, B. A., and MAY, V. M. (1966).—Brookhaven National Lab. Rep. No. BNL 325, 2nd Ed., Suppl. No. 2.
- KAVALOSKI, C. D., and KOSSLER, W. J. (1969).—*Phys. Rev.* **180**, 971.
- LANE, A. M., and LYNN, J. E. (1960).—*Nucl. Phys.* **17**, 586.
- MOXON, M. D. (1965).—Proc. Int. Conf. on Study of Nuclear Structure with Neutrons, Antwerp, p. 338.
- TRIPATHI, K. C., BLICHERT, P. H., and BOREVINGS, S. (1969).—Proc. Int. Symp. on Neutron Capture Gamma-ray Spectroscopy, Studsvik, p. 183. (IAEA: Vienna.)

